Comparison of Reconstruction Algorithms for Brain Stroke Microwave Imaging

Comparison of Reconstruction Algorithms for Brain Stroke Microwave Imaging

Valeria Mariano
Dept. of Electronics and Telecommunications (DET)
Politecnico di Torino
Torino, Italy
valeria_mariano@polito.it

Jorge Alberto Tobon Vasquez
Dept. of Electronics and Telecommunications (DET)
Politecnico di Torino
Torino, Italy
tobonjorge@gmail.com

Rosa Scapaticci
Institute for the Electromagnetic Sensing of the Environment
Nationale Research Council
Napoli, Italy
scapaticci.r@irea.cnr.it

Lorenzo Crocco
Institute for the Electromagnetic Sensing of the Environment
Nationale Research Council
Napoli, Italy
crocco.l@irea.cnr.it

Panagiotis Kosmas
Dept. of Informatics, Fac. of Natural & Mathematical sciences
Kings College London (KCL)
London United Kingdom
panagiotis.kosmas@kcl.ac.uk

Francesca Vipiana
Dept. of Electronics and Telecommunications (DET)
Politecnico di Torino
Torino, Italy
francesca.vipiana@polito.it

***Abstract*—The aim of this paper is to describe and compare the performances of three image reconstruction algorithms that can be used for brain stroke microwave imaging. The algorithms belong to the class of non-linear iterative algorithms and are capable of providing a quantitative map of the imaged scenario. The first algorithm is the Contrast Source Inversion (CSI) method, which uses the Finite Element Method (FEM) to discretize the domain of interest. The second one is the Subspace-Based Optimization Method (SOM) that has some properties in common with the CSI method, and it also uses FEM to discretize the domain. The last one is the Distorted Born Iterative Method with the inverse solver Two-step Iterative Shrinkage/Thresholding (DBIM-TwIST), which exploits the forward Finite Difference Time Domain (FDTD) solver. The reconstruction examples are created with 3-D synthetic data modelling realistic brain tissues with the presence of a blood region, representing the stroke area in the brain, whereas the inversion step is carried out using a 2-D model.**

Keywords—microwave imaging, brain stroke imaging, Contrast Source Inversion (CSI) method, Subspace-Based Optimization Method (SOM), Distorted Born Iterative Method (DBIM).

I. INTRODUCTION

Brain stroke is one of the most widespread cardiovascular diseases and it can lead to permanent paralysis, to disability and, in the worst case, to death. There are two types of stroke: the ischemic stroke, when a brain vessel is clogged, and the haemorrhagic stroke, when a brain vessel bursts. In both cases, the effectiveness of treatments depends on the intervention time as the patient condition can drastically worsen very quickly. For these reasons, there is the need of a technique that allows a real-time and continuous monitoring of the bedridden patient.

Nowadays, the main diagnostic techniques for clinician's support are Magnetic Resonance Imaging (MRI) and Computerized Tomography (CT). However, these techniques are not viable for continuous monitoring because both are bulky and not portable, so the bedridden patient must be moved to the exam room. Moreover, MRI is very expensive and inaccessible for claustrophobic patient, instead CT is invasive and harmful for the patient, especially if repeated several times. An interesting technique, complementary to the once already available, is Microwave Imaging (MWI). The basic concept of this method is that microwaves are sensitive to different electrical permittivity and thanks to the dielectric contrast between abnormal blood flow or reduced oxygen tissues with respect to healthy tissues, then it is possible to obtain quantitative parameters and to classify different type of strokes. The MWI device is composed by a data acquisition block with an antennas array, connected to a processing block (the entire set up is described in e.g. [1]). Examples of MWI systems are in [2], [3], [4] and [5]. In this paper, the processing block is analysed, in particular the aim is the comparison among different image reconstruction algorithms: the Contrast Source Inversion (CSI) method [6], the Subspace-Based Optimization Method (SOM) [7] and the Distorted Born Iterative Method with the inverse solver Two-step Iterative Shrinkage/Thresholding (DBIM-TwIST), the last one implemented by KCL [8]. The algorithms are used to reconstruct 2-D image from synthetic 3-D data, simulated with an in-house FEM-based solver, representing a brain stroke scenario.

This work was supported by the Italian Ministry of University and Research under the PRIN project MiBraScan - Microwave Brain Scanner for Cerebrovascular Diseases Monitoring

978-1-7281-5866-2/20/$31.00 ©2020 IEEE

II. THEORETICAL FOUNDATION

The CSI method, the SOM and the DBIM-TwIST belong to the class of non-linear iterative reconstruction algorithms. In this section, a brief description of the three algorithms in a 2-D scalar scattering problem is given (TM case). The Object of Interest (OI) is located in an imaging domain D and it is immersed in a background medium (possibly inhomogeneous) with known electrical properties. An array of antennas surrounds the domain D, acting both transmitters and receivers. Accordingly, when one of the antennas illuminates the domain D, the others measure the field. In the absence of the OI, the measured field is called incident field, instead when there is the OI, it is called total field. The difference between the total and the incident field is the scattered field and conveys the information on the contrast between the OI and the background dielectric properties, which represents the unknown of the problem. The contrast is:

$$\chi(\boldsymbol{r}) = (\varepsilon_r(\boldsymbol{r}) - \varepsilon_b(\boldsymbol{r}))/\ \varepsilon_b(\boldsymbol{r}) \tag{1}$$

where, $\varepsilon_b(\boldsymbol{r})$ and $\varepsilon_r(\boldsymbol{r})$ are respectively the background and the OI complex permittivity, with $\boldsymbol{r} = (x, y)$ [7].

A. Contrast Source Inversion (CSI) method

The CSI method solves the inverse scattering problem without the explicit need of computing the forward solution at each iteration. The CSI introduces the contrast sources w that relates the contrast and the total field:

$$w_t(\boldsymbol{r}) := \chi(\boldsymbol{r})\ E_t(\boldsymbol{r}) \tag{2}$$

where, $E_t(\boldsymbol{r})$ is the total field (in z-direction) in $\boldsymbol{r}$ when the transmitter t illuminates the domain D. In our implementation the Finite-Element Method (FEM) is used to discretize the 2-D domain, therefore we can have boundaries of any type and shape. The mesh is conformal, non-uniform and unstructured and is composed by triangular elements. The CSI looks for OI dielectric properties by minimizing a cost functional:

$$F^{CSI}(\chi, w_t) = F^S(w_t) + F^D(\chi, w_t) \tag{3}$$

where $F^S(w_t)$ and $F^D(\chi, w_t)$ are respectively the data error and the object error functional. The complete formulation is described in [6]. The cost functional (3) is minimized updating alternatively the contrast sources and the contrast variable. The former is updated exploiting the conjugate-gradient (CG) method with Polak-Ribière search directions (in this section χ is constant), instead χ is updated minimizing the object error functional (with w_t constant) [6]. Here, the CSI method is implemented without any type of regularization.

B. Subspace-Based Optimization Method (SOM)

The SOM inherits some parts from the CSI method. In this algorithm, the contrast sources variable is divided into two parts: the deterministic part (w^s) that is obtained from the spectrum analysis, and the ambiguous part (w^n) that is calculated with optimization. As described in [7], in order to obtain the contrast sources, it is necessary to compute the Singular Value Decomposition (SVD) of the operator G_S ($G_S = \Sigma_m\, u_m \sigma_m v_m^*$), that links the contrast sources variable to the scattered field:

$$w^s = \sum_j^L (u_j\, E^{sca}\, v_j)/\ \sigma_j \tag{4}$$

where E^{sca} is the scattered field, u and v are respectively the left and right singular vector, σ is the singular value and L is the number of values that are under a defined threshold of noise. The ambiguous part is defined as $w^n = V^n \alpha^n$, where V^n is a matrix composed by the remaining M – L right vectors (M is the total number of subunits in which the domain of interest is divided), and α^n is the unknown M – L vector. The cost functional is very similar to the CSI method one, and in this case, it is minimized updating α^n and χ [7].

C. Distorted Born Iterative Method (DBIM)

The DBIM algorithm solves the inverse scattering problem creating, at each iteration and for each transmitter-receiver pair, a linear equation under the Born approximation. In this way, it creates a linear system that can be solved with different methods [8]. The method used in this case is the Two-step Iterative Shrinkage/Thresholding (TwIST) that has to find an unknown vector $\boldsymbol{x}$ (original image), from a vector $\boldsymbol{y}$ (observation vector), linked together by the linear equation $\boldsymbol{Ax} = \boldsymbol{y}$, where $\mathbf{A}$ is a linear operator. The unknown $\boldsymbol{x}$ is a minimiser of a convex objective function as explained in [8]. To be more stable, the TwIST method computes the current iteration as function of the two previous once: it has a faster convergence and the reconstruction are more accurate than one-step iterative methods. The two-step iterative equation is reported below:

$$\boldsymbol{x}_{t+1} = (1-\alpha)\,\boldsymbol{x}_{t-1} + (\alpha - \beta)\,\boldsymbol{x}_t + \beta\,\Gamma_\lambda(\boldsymbol{x}_t)$$

$$\Gamma_\lambda(\boldsymbol{x}) = \Psi_\lambda(\boldsymbol{x} + \boldsymbol{A}^T(\boldsymbol{y} - \boldsymbol{A}\boldsymbol{x})) \tag{5}$$

where $\boldsymbol{x}_{t+1}$, $\boldsymbol{x}_t$ and $\boldsymbol{x}_{t-1}$ are the variable respectively at next, current and previous evaluation. α and β are TwIST parameters and Ψ_λ is the regularization operator. The DBIM exploits the forward FDTD solver [8].

III. ALGORITHMS COMPARISON

In this section, the algorithms' performances are compared using 3-D synthetic data. The model created in an external CAD-mesh software is reported in Fig. 1; it is composed by a simplified brain phantom (dielectric properties equal to the average of dielectric properties of brain tissues) immersed in a background medium and surrounded by 12 antennas. The target is located in an asymmetric position in the phantom and mimics the dielectric properties of a haemorrhagic stroke. The simulation data are obtained with a 3-D in-house FEM. All the materials properties are obtained with the measurement system described in [5]. In order to choose the working frequency range is fundamental to analyse the transmission coefficient of the field through the head tissues as function of frequency and relative permittivity of the background medium. As described in [5], there is a range of frequency with low transmission, so we choose a frequency lower than about 1.5 GHz or higher than about 2.5 GHz. As penetration at higher frequencies is limited by losses, we select a frequency around 1 GHz and a background medium composed by Triton X-100 and water in percentage 70/30. Fig. 2 shows S_{11} parameters as function of frequency (from 0.5 to 1.5 GHz) for an antenna immersed in the

background medium (the 3D model is created in the CAD-mesh software and the synthetic S parameters are obtained with an in-house FEM). The antenna has a resonance in 1.1 - 1.15 GHz. Since the simulation are created with an external software a fundamental step is calibration [9]

$$E^{Cal,\ target} = (E^{Ref,\ not\ target} / S^{Sim,\ not\ target})\ S^{Sim,\ target} \qquad (6)$$

where $S^{Sim,\ not\ target}$ and $S^{Sim,\ target}$ are the synthetic data respectively without and with the target, $E^{Ref,\ not\ target}$ are the data created with the forward solvers internal to the algorithms (FEM for CS and SOM, and FDTD for DBIM) without the target. Fig. 3 shows the values of synthetic data before and after calibration when the antenna 3 transmits for the FEM data (CS/SOM) and FDTD data (DBIM-TwIST). One can notice that after calibration the synthetic data are almost totally overlapping to the reference one. In Fig. 4 and 5, the reconstruction obtained respectively for permittivity and conductivity are depicted (with a frequency of 1.1 GHz). All the algorithms achieved good results: the shape and position of the target are correctly estimated (small red circle identifies the right position) and the values of permittivity and conductivity are very close to the actual ones, as reported in Table I that contains the average values. Moreover, the computational time is comparable. However, reconstruction of conductivity of CSI method (Fig. 5a) and SOM (Fig. 5b) have some inaccuracy that can be overcome using regularization.

IV. Conclusion and Perspectives

In this paper, MWI reconstruction algorithms have been compared using 3-D synthetic data. The algorithms provide comparable results, with a slightly better outcome for DBIM, possibly due to the fact no regularization was enforced in the CS and SOM implementation. Future work deals with the use of regularization strategies to improve the performance of the algorithms as well as with the efficient 3-D implementation, in order to carry out a validation with experimental data measured with a 3-D helmet-like system [10]. Possible extra results, as 3-D extension, will be presented in the conference.

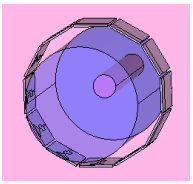

Fig. 1. Model geometry realized in a CAD-mesh software

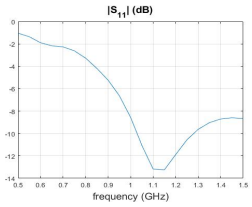

Fig. 2. S parameters of an antenna immersed in the background medium (synthetic data)

TABLE I. Blood Dielectric Permittivity

Dielectric properties	Expected	CS	SOM	DBIM-TwIST
Permittivity	63.06	50.45± 4.13	48.87± 6.26	53.90± 5.77
Conductivity (S/m)	1.62	1.10 ± 0.20	1.01 ± 0.25	1.21 ± 0.14

Acknowledgment

The DBIM-TwIST code was provided by Olympia Karadima, KCL (London, UK).

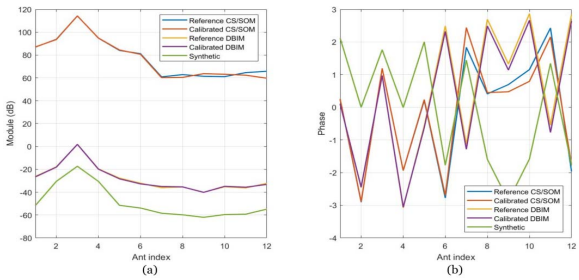

Fig. 3. Calibration effect. (a) Module and (b) Phase of synthetic data before calibration, synthetic data after calibration (FEM and FDTD) and reference data (FEM and FDTD).

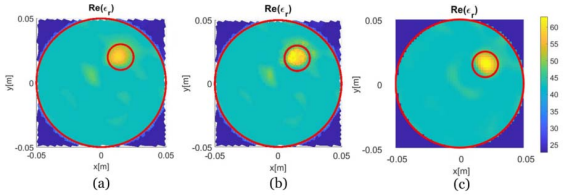

Fig. 4. Permittivity. (a) CSI method, (b) SOM and (c) DBIM-TwIST.

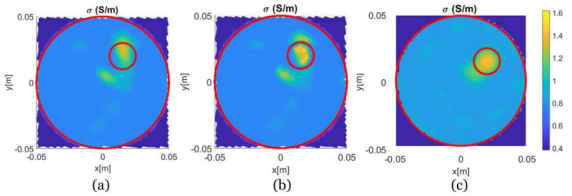

Fig. 5. Conductivity. (a) CSI method, (b) SOM and (c) DBIM-TwIST.

References

[1] R. Scapaticci, J. Tobon, G. Bellizzi, F. Vipiana, L. Crocco, "Design and numerical characterization of a low-complexity microwave device for brain stroke monitoring," IEEE Trans. Antennas Propag., vol. 66, pp. 7328–7338, Dec. 2018.

[2] A. Fhager, S. Candefjord, M. Elam, M. Persson, "Microwave diagnostics ahead: Saving time and the lives of trauma and stroke patients," IEEE Microwave Mag., vol. 19, no. 3, pp. 78–90, May 2018.

[3] M. Hopfer, R. Planas, A. Hamidipour, T. Henriksson, S. Semenov, "Electromagnetic tomography for detection, differentiation, and monitoring of brain stroke: A virtual data and human head phantom study." IEEE Ant. Propag. Mag., vol. 59, no. 5, pp. 86–97, Oct. 2017.

[4] A. T. Mobashsher and A. M. Abbosh, "On-site rapid diagnosis of intracranial hematoma using portable multi-slice microwave imaging system," Scientific Reports, vol. 6, pp. 1–17, Nov. 2016.

[5] J. A. Tobon et al., "Design and Experimental Assessment of a 2D Microwave Imaging System for Brain Stroke Monitoring," Hindawi, vol 2019, Article ID 8065036, 12 pages.

[6] A. Zakaria, C. Gilmore, and J. LoVetri, "Finite-element contrast source inversion method for microwave imaging," Inverse Prob., vol. 26, no. 11, p. 115010, 2010.

[7] Xudong Chen, "Subspace-Based Optimization Method for Solving Inverse Scattering Problems," IEEE Trans. on Geoscience and Remote Sensing, vol. 48, NO.1, January 2010.

[8] Z. Miao and P. Kosmas, "Multiple-frequency DBIM-TwIST algorithm for microwave breast imaging," IEEE Trans. on Antennas and Propag., 65(5):2507–2516, May 2017.

[9] M. Ostadrahimi, et al., ''Analysis of incident field modeling and incident/scattered field calibration techniques in microwave tomography,'' IEEE Antennas and Wirless Propag. Letters, vol. 10, pp. 900–903, 2011.

[10] J. A. Tobon et al., "Portable 3-D Microwave Imaging System for Cerebrovascular Diseases Monitoring," 14th European Conference on Antennas and Propag., EuCAP 2020, in Copenhagen, Denmark, March 15-20, 2020.